Below and above bandgap excited photoluminescence in $Tl_4InGa_3S_8$ layered single crystals

2007 J. Phys.: Condens. Matter 19 456221

(http://iopscience.iop.org/0953-8984/19/45/456221)

IOP PUBLISHING JOURNAL OF PHYSICS: CONDENSED MATTER

J. Phys.: Condens. Matter **19** (2007) 456221 (10pp) doi:10.1088/0953-8984/19/45/456221

Below and above bandgap excited photoluminescence in $Tl_4InGa_3S_8$ layered single crystals

K Goksen and N M Gasanly[1]

Physics Department, Middle East Technical University, 06531 Ankara, Turkey

E-mail: nizami@metu.edu.tr (N M Gasanly)

Received 23 July 2007, in final form 27 August 2007
Published 22 October 2007
Online at stacks.iop.org/JPhysCM/19/456221

Abstract

Photoluminescence (PL) spectra of $Tl_4InGa_3S_8$ layered single crystals grown by the Bridgman method have been studied in the 550–710 nm wavelength and 80–300 K temperature ranges with below bandgap excitation ($\lambda_{exc} = 532$ nm), and in the 420–600 nm wavelength and 30–300 K temperature ranges with above bandgap excitation ($\lambda_{exc} = 325$ nm). The broad emission bands centered at 580 nm (2.14 eV) and 496 nm (2.49 eV) were observed at $T = 80$ and 30 K for below and above bandgap excitation processes, respectively. Variations in emission spectra have been studied as a function of excitation laser intensity in the 10.3–429.7 mW cm^{-2} range for below bandgap excitation. Radiative transitions from the donor levels located at 0.02 and 0.37 eV below the bottom of the conduction band to the deep acceptor level located at 0.20 eV above the top of the valence band were proposed to be responsible for the observed PL bands. From x-ray powder diffraction and EDS analysis, the monoclinic unit cell parameters and compositional parameters, respectively, were determined.

1. Introduction

The quaternary $Tl_4InGa_3S_8$ crystal belongs to the group of layered semiconductors. This compound is a structural analog of $TlGaS_2$, in which a quarter of the gallium ions are replaced by indium ions [1, 2]. The lattice of $Tl_4InGa_3S_8$ consists of strictly periodic two-dimensional layers arranged parallel to the (001) plane (figure 1). Each successive layer is rotated by a right angle with respect to the previous one. Interlayer bonding is formed between Tl and S atoms while the bonding between Ga(In) and S atoms is an intralayer type. The fundamental structural unit of a layer is the $Ga_4(In_4)S_6$ adamantane-like units linked together by bridging S atoms.

The optical and photoelectrical properties of $TlGaS_2$ layered crystals were studied in [3–8]. The fundamental absorption edges are formed by indirect and direct transitions with

[1] Author to whom any correspondence should be addressed.

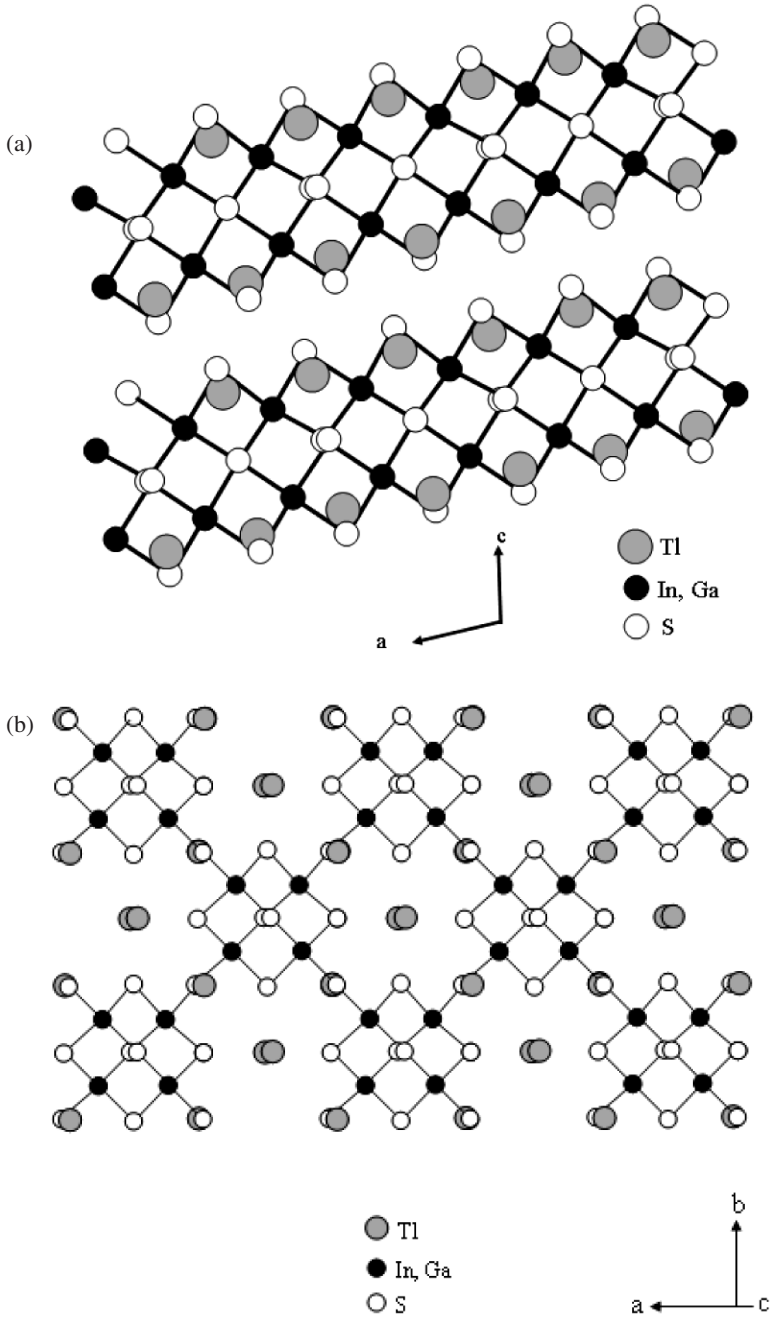

Figure 1. Projection of the crystal structure of $Tl_4InGa_3S_8$ on *ac*-planes (a) and *ab*-planes (b).

$E_{gi} = 2.38$ eV and $E_{gd} = 2.53$ eV at room temperature [3]. A high photosensitivity in the visible range of spectra and high birefringence in conjunction with a wide transparency range of 0.5–14 μm make these crystals useful for optoelectronic applications [8]. Previously, we studied the temperature-dependent photoluminescence (PL) spectra of $TlGaS_2$ and Tl_2InGaS_4

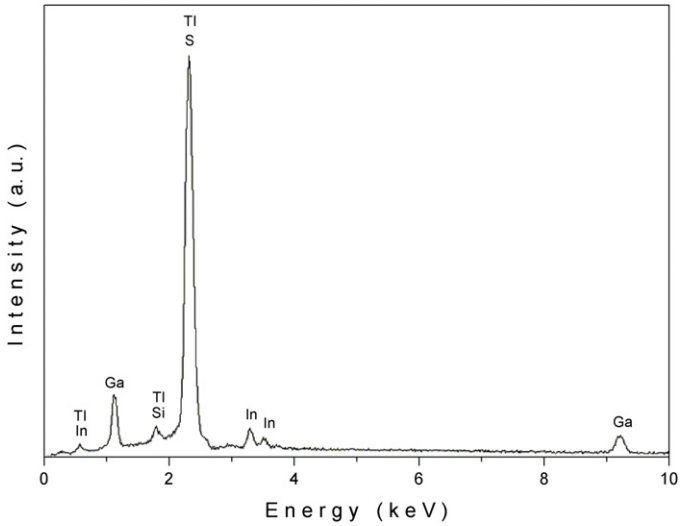

Figure 2. EDS analysis of $Tl_4InGa_3S_8$ crystal.

crystals and observed three broad emission bands centered at 568, 718 and 1102 nm ($TlGaS_2$) and 542, 607 and 707 nm (Tl_2InGaS_4), which were assigned to the radiative transitions from donor levels located below the bottom of conduction band to acceptor levels located above the top of the valence band [9, 10]. Moreover, we have recently studied the optical properties of $Tl_4InGa_3S_8$ crystals by means of transmission and reflection measurements in the wavelength range of 400–1100 nm [11]. Analysis of the room temperature absorption data revealed the presence of both optical indirect and direct transitions with bandgap energies of 2.40 and 2.61 eV, respectively. Transmission measurements carried out in the temperature range of 10–300 K revealed the rate of change of the indirect bandgap with temperature as $\gamma = -6.8 \times 10^{-4}$ eV K^{-1}. The dispersion of the refractive index was discussed in terms of the Wemple–DiDomenico single-effective-oscillator model.

In the present paper, we report the results of x-ray analysis in the 10°–80° diffraction angle (2θ) range for $Tl_4InGa_3S_8$ crystals. The lattice parameters were determined by x-ray measurements, while the compositional parameters of the crystal were determined by energy dispersive spectroscopic (EDS) analysis. The variations in the PL emission bands for below and above bandgap excitation processes were studied as a function of temperature in 80–300 K and 30–300 K ranges, respectively. The dependence of PL spectra on laser excitation intensity was also studied for below bandgap excitation process. As a result of the analysis, the origin of both emission bands was suggested to be recombination of charge carriers from donor to acceptor states.

2. Experimental details

Single crystals of $Tl_4InGa_3S_8$ were grown by the Bridgman method. The resulting ingot appeared green in color and the freshly cleaved surfaces were mirror-like. The chemical compositions of $Tl_4InGa_3S_8$ crystal was determined by EDS analysis using a JSM-6400 electron microscope (figure 2). The atomic composition ratio of the investigated sample (Tl:In:Ga:S) was found to be 26.1:6.1:19.0:48.8, respectively. Moreover, EDS analysis revealed that silicon impurity was present in the studied crystals. The fractional amount of the impurity was estimated to be somewhat less than 0.1–0.2%.

Table 1. X-ray powder diffraction data for $Tl_4InGa_3S_8$ crystals.

No.	*hkl*	d_{obs} (nm)	d_{calc} (nm)	I/I_0
1	1 0 $\bar{1}$	0.7456	0.7460	3
2	2 0 $\bar{2}$	0.3739	0.3737	100
3	1 1 $\bar{1}$	0.3648	0.3651	6
4	2 1 $\bar{1}$	0.3285	0.3284	3
5	1 1 1	0.3134	0.3133	2
6	2 1 $\bar{2}$	0.2789	0.2789	15
7	3 0 $\bar{3}$	0.2494	0.2493	8
8	0 0 3	0.2304	0.2305	3
9	4 0 $\bar{4}$	0.1870	0.1871	12
10	1 2 $\bar{2}$	0.1841	0.1841	3
11	2 1 $\bar{4}$	0.1753	0.1753	4
12	2 1 3	0.1650	0.1650	6
13	7 1 0	0.1330	0.1330	3
14	8 0 0	0.1227	0.1227	2

For the x-ray powder diffraction experiments, a Philips PW1740 diffractometer with monochromatized Cu Kα radiation ($\lambda = 0.154\,049$ nm) was used at a scanning speed of 0.02° s^{-1}. Crystals suitable for PL measurements had typical sample dimensions of $6 \times 4 \times 1$ mm^3. The electrical conductivity of the studied sample was determined as n-type. The green line ($\lambda = 532$ nm) of a continuous frequency-doubled YAG:Nd^{3+} laser (below bandgap excitation) and the 325 nm line of a He–Cd laser (above bandgap excitation) were used as the excitation light sources. PL experiments were carried out by collecting the light from the laser-illuminated face of the sample in a direction close to the normal of the layer. A CTI-Cryogenics M-22 closed-cycle helium cryostat was used to cool the sample from room temperature down to 30 K, and the temperature was controlled within an accuracy of ±0.5 K. The PL spectra of the sample in the region 420–710 nm were analyzed using a Oriel MS-257 grating monochromator and Hamamatsu S7010-1008 FFT-CCD image sensor with single stage electric cooler. Sets of neutral density filters were used to adjust the exciting laser ($\lambda_{exc} = 532$ nm) intensity from 10.3 to 429.7 mW cm^{-2}. All measured PL spectra have been corrected for the spectral response of the optical apparatus.

3. Results and discussion

The Miller indices (*hkl*), the observed and calculated interplanar spacings (*d*) and the relative intensity (I/I_0) of the diffraction lines of $Tl_4InGa_3S_8$ crystal were obtained from room temperature x-ray powder diffraction experiments (table 1). The lattice parameters of the monoclinic unit cell, calculated by using a least squares computer program DİCVOL 04 were found to be $a = 0.7777$, $b = 0.4192$ and $c = 1.0198$ nm, and $\beta = 105.63°$.

Temperature-dependent PL measurements in $Tl_4InGa_3S_8$ crystal were carried out by using two different excitation sources. Since our sample has a direct bandgap of $E_g = 2.71$ eV at $T = 30$ K [11], the source (He–Cd laser) with $\lambda_{exc} = 325$ nm (3.82 eV) is referred to as the above bandgap excitation source and the other one (YAG:Nd^{3+} laser) with $\lambda_{exc} = 532$ nm (2.33 eV) is referred to as the below bandgap excitation source, for this study. Figure 3 shows PL spectra of a $Tl_4Ga_3InS_8$ crystal corresponding to the above bandgap excitation process in the 420–600 nm wavelength region and the 30–300 K temperature range at a constant excitation laser intensity of 2476.4 mW cm^{-2}. Figure 4 demonstrates PL spectra of the sample

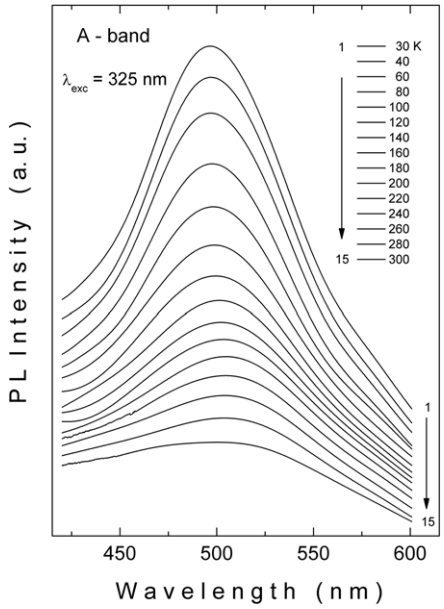

Figure 3. Temperature dependence of PL spectra of $Tl_4InGa_3S_8$ crystal for above bandgap excitation with $\lambda_{exc} = 325$ nm at an excitation laser intensity of $L = 2476.4$ mW cm^{-2}.

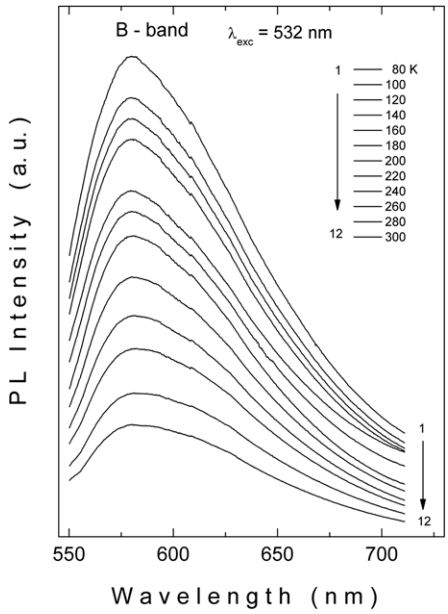

Figure 4. Temperature dependence of PL spectra of $Tl_4InGa_3S_8$ crystal for below bandgap excitation with $\lambda_{exc} = 532$ nm at an excitation laser intensity of $L = 429.7$ mW cm^{-2}.

corresponding to the below bandgap excitation process in the 550–710 nm wavelength region and 80–300 K temperature range at a constant excitation laser intensity of 429.7 mW cm^{-2}. In figure 3, a broad emission band having a full-width at half maximum (FWHM) of 0.53 eV at

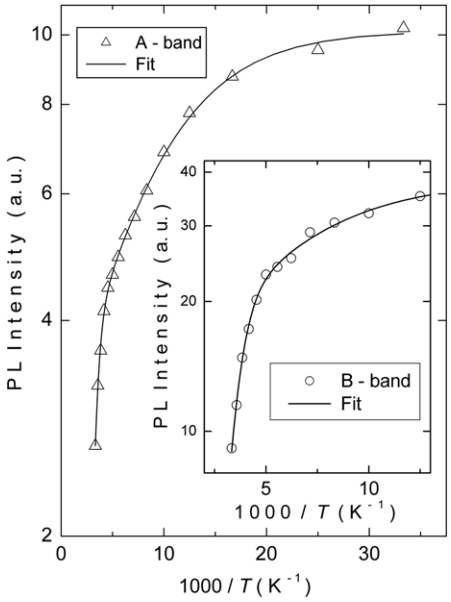

Figure 5. Temperature dependences of PL intensities at emission band maxima for A- and B-bands.

$T = 30$ K centered at 496 nm (2.49 eV, A-band) was observed, while in figure 4 another broad emission band with FWHM of 0.25 eV at $T = 80$ K centered at 580 nm (2.14 eV, B-band) was revealed. These large FWHM values of A- and B-bands are typical properties of emissions originating from donor–acceptor pair transitions [12]. From figures 3 and 4, it is also clear that both band peak energies show a red shift of different degrees. The change in the peak energy of the A-band with increasing temperature from 30 to 300 K is about 80 meV, whereas that of the B-band in the temperature interval of 80–300 K is about 6 meV.

The temperature dependence of the peak intensity of the PL spectra can also be used to obtain valuable information about the electronic energy levels in the forbidden energy gap. Figures 3 and 4 show that the peak intensities of both A- and B-bands change as a function of sample temperature. To analyze the intensity behavior of both bands, the Arrhenius plots of peak intensity dependence on temperature are plotted in figure 5. From the figure it is clear that as the temperature is increased both bands significantly decrease in intensity. It is well-known that the decrease in intensity can be explained by the activation of nonradiative processes in the crystal structure. From the figure it is also seen that neither band has completely vanished at 300 K, therefore, before doing any calculations, we supposed that the activation energies for both bands should have been large enough to completely overcome quenching at room temperature, which can also be interpreted to show that we are dealing with deep defect levels. The thermal quenching behavior of PL peak intensity can be defined best by the following equation with two activation energies [13]:

$$I(T) = \frac{I_0}{1 + \alpha_1 \exp(-E_1/kT) + \alpha_2 \exp(-E_2/kT)}, \tag{1}$$

where I is the PL intensity, I_0 is a proportionality constant, k is Boltzmann's constant, α_1 and α_2 are process rate parameters and E_1 and E_2 are the activation energies of nonradiative processes in the low- and high-temperature regions, respectively. The activation energies for both bands have been obtained by fitting experimental data to the equation (1). The results of the fits are

shown in figure 5. After a successful fitting process, it was found that the A-band quenches with two activation energies as $E_{1A} = 0.02$ eV at low temperatures and $E_{2A} = 0.20$ eV at higher temperatures, while the B-band also quenches with two activation energies as $E_{1B} = 0.03$ eV at low temperatures and $E_{2B} = 0.20$ eV at higher temperatures. From the results, it is clear that the activation energies E_{2A} and E_{2B} belong to the same energy level, therefore we can say that the origin of both emission processes is the same energy level having an activation energy of 0.20 eV, which also confirms our previous remark that a deep defect level plays a role in both emissions processes. Here, it is necessary to recall the general expression for emission energy of a donor–acceptor pair as [12]

$$h\nu = E_g - E_a - E_d, \tag{2}$$

where E_g is the bandgap energy of $Tl_4Ga_3InS_8$ crystal and E_a and E_d are the donor and acceptor level energies, respectively. A simple calculation with equation (2) for A-band emission by using the values of $E_g = 2.71$ eV, $h\nu_A = 2.49$ eV and $E_a(E_{2A}) = 0.20$ eV gives us the energy of the donor level $E_d(E_{1A})$ as 0.02 eV. Moreover, since $Tl_4InGa_3S_8$ crystal has n-type conductivity, it is very reasonable to believe that the A-band low-temperature activation energy E_{1A} relates to the shallow donor level d_1 located below the conduction band at 0.02 eV, which also confirms our previous calculation result. On the other hand, we notice that the B-band low-temperature activation energy E_{1B} does not simply belong to a shallow donor level. The reason for this proposition is that the thermal quenching process of the B-band cannot be described by the existence of a 0.03 eV shallow donor level, since equation (2) is not satisfied with obtained values of $E_g = 2.71$ eV, $h\nu_B = 2.14$ eV, E_d $(E_{1B}) = 0.03$ eV and E_a $(E_{2B}) = 0.20$ eV. Therefore, we suppose the presence of two deep donor levels d_2 and d_3 with energies 0.34 and 0.37 eV, respectively, in the band gap. In this case, the activation energy $E_{1B} = 0.03$ eV actually corresponds to the thermal release of electrons from the deep donor state d_3 to the shallower state d_2. A similar proposal for two close deep acceptor levels in CdTe crystal has been made by Cotal *et al* [14], where the low-temperature activation energy (0.02 eV) was directly related to the thermal quenching process between these deep acceptor levels.

Excitation laser intensity dependence of the PL spectra is an important consideration when studying the nature of deep level luminescence from semiconductors. For this reason, to study excitation laser intensity-dependent variations of the B-band, the PL measurements were done at $T = 80$ K in the 10.3–429.7 mW cm^{-2} excitation laser intensity range and the 540–710 nm wavelength region with only below bandgap excitation using a YAG:Nd^{3+} laser. The excitation laser intensity dependence of the A-band with above bandgap excitation could not be studied due to a lack of neutral density filters that can be used at $\lambda_{exc} = 325$ nm. The results of the experiments for different excitation laser intensities are shown in figure 6. From the figure, it is easily noticeable that the B-band peak intensity changes as a function of excitation laser intensity, whereas its energy does not show any significant change at all. This kind of behavior can be explained by a closely spaced donor–acceptor pair model, which proposes that the donor–acceptor pairs responsible for the emission are located at only closely spaced sites and are distributed homogeneously, in contrast with inhomogeneously distributed donor–acceptor pairs where increasing laser intensity excites more pairs that are closely spaced leading to a blue shift of the peak energy of the observed band [12]. We believe that these pairs are associated with some uncontrollable defects in the crystal structure due to stacking faults or unintentional impurities. Further analyses were carried out by fitting the experimental data to a power law of the form

$$I \propto L^{\gamma}, \tag{3}$$

where I is the PL intensity, L is the excitation laser intensity and γ is a dimensionless exponent. It was revealed that the intensity of the B-band increases sublinearly with increasing excitation

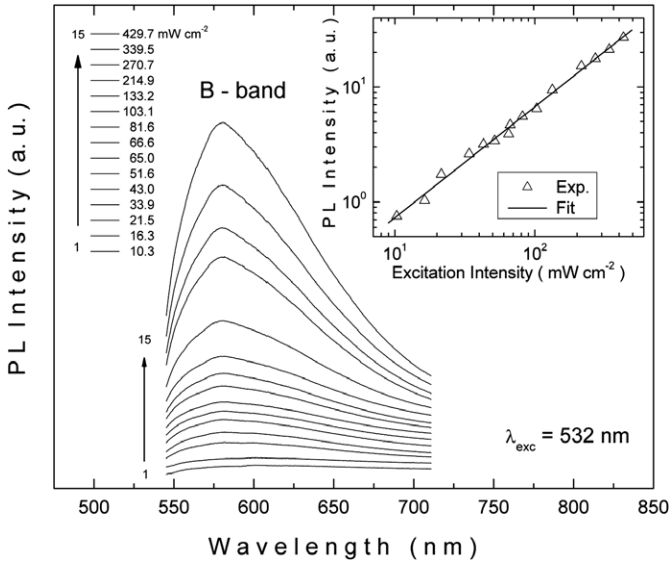

Figure 6. Excitation laser intensity dependence of PL spectra of $Tl_4InGa_3S_8$ crystal for below bandgap excitation with $\lambda_{exc} = 532$ nm at $T = 80$ K. Inset: dependence of B-band PL intensity at the emission band maxima on the excitation laser intensity ($\lambda_{exc} = 532$ nm).

laser intensity. The value of γ was found to be 0.96 by a linear fit, as shown in the inset to figure 6. It is well-known that the coefficient γ is generally $1 < \gamma < 2$ for the free- and bound-exciton emission, and $\gamma < 1$ for free-to-bound and donor–acceptor pair recombinations [15]. Thus, the obtained value of $\gamma < 1$ further confirms our assertion that the B-band originates from a donor–acceptor pair recombination.

As a result of the analysis, we propose a band structure model for $Tl_4InGa_3S_8$ crystal, presented in figure 7. In this model, one shallow donor level d_1 and two deep donor levels d_2 and d_3 are located at 0.02 eV, 0.34 eV and 0.37 eV, respectively, below the conduction band. In addition to these donor levels, we also suppose that a deep acceptor level a is located at 0.20 eV above the valence band. Taking into account the high resistivity of our crystal, we believe that the concentration of acceptors is high enough to efficiently compensate the donors. At this point, it is inevitable that the below bandgap excitation with photons from the YAG:Nd^{+3} laser having a wavelength of $\lambda_{exc} = 532$ nm (2.33 eV) does not have enough energy to overcome the bandgap energy, so such an excitation can only cause the electrons to be excited from the acceptor level a to levels above the deep donor levels. Then the excited electrons make a transition from the donor level d_3 to the acceptor level a, giving rise to B-band emission. When we switch to above bandgap excitation with photons from the He–Cd laser having a wavelength of $\lambda_{exc} = 325$ nm (3.82 eV), it is seen that the photon energy is high enough to overcome the bandgap energy this time. So, the electrons can easily be excited to the conduction band. If the transition probability between the shallow donor level and the deep acceptor level is greater than that of the deep donor level and deep acceptor level, the dominant radiative recombination will occur from the shallow donor level to the deep acceptor level. Therefore, transitions from the donor level d_1 to the acceptor level a result in A-band emission. In such a condition, B-band emission is not observed in the spectra due to its relatively low probability, as expected.

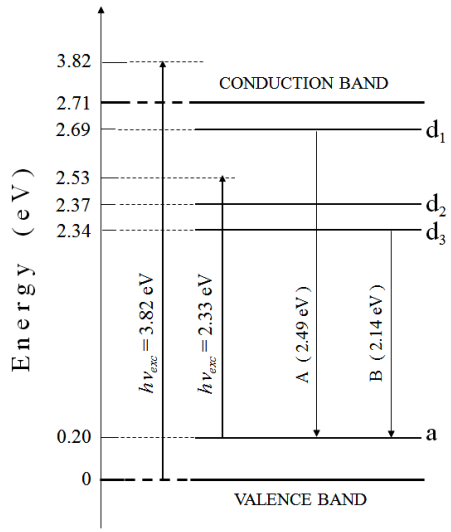

Figure 7. Proposed band model for $Tl_4InGa_3S_8$ crystal.

4. Conclusions

$Tl_4InGa_3S_8$ crystals were characterized by x-ray powder diffraction and EDS analysis. The parameters of the monoclinic unit cell were found to be $a = 0.7777$, $b = 0.4192$ and $c = 1.0198$ nm, and $\beta = 105.63°$, while the atomic composition ratio of the studied samples (Tl:In:Ga:S) was determined as 26.1:6.1:19.0:48.8, respectively. The dependences of PL spectra of $Tl_4InGa_3S_8$ crystals on temperature and excitation laser intensity were studied in the wavelength range of 420–710 nm. The visible emission bands centered at 496 nm (2.49 eV) and 580 nm (2.14 eV) were observed for above and below bandgap excitation processes, respectively. The variations of the emission spectra with respect to temperature and excitation laser intensity revealed that the centers responsible for the emissions were donor and acceptor levels. In the case of photoluminescence under below bandgap excitation, the peak energy does not show any variance under increasing laser excitation intensity, which means that the recombination process is only due to closely spaced pairs. As the studied crystals were not intentionally doped, the donor and acceptor states are thought to originate from unintentional impurities and stacking faults or point defects created during crystal growth.

References

[1] Muller D and Hahn H 1978 *Z. Anorg. Allg. Chem.* **438** 258
[2] Yee K A and Albright A 1991 *J. Am. Chem. Soc.* **113** 6474
[3] Hanias M, Anagnostopoulos A, Kambas K and Spyridelis J 1992 *Mater. Res. Bull.* **27** 25
[4] Kato A, Nishigaki M, Mamedov N, Yamazaki M, Abdullaeva S, Kerimova E, Uchiki H and Iida S 2003 *J. Phys. Chem. Solids* **64** 1713
[5] Ashraf I M 2004 *J. Phys. Chem.* **108** 10765
[6] Karabulut O, Parlak M and Mamedov G M 2007 *J. Alloys Compounds* **429** 50
[7] Kashida S, Yanadori Y, Otaki Y, Seki Y and Panich A M 2006 *Phys. Status Solidi* a **203** 2666
[8] Allakhverdiev K R 1999 *Solid State Commun.* **111** 253
[9] Yuksek N S, Gasanly N M, Aydinli A, Ozkan H and Acikgoz M 2004 *Cryst. Res. Technol.* **39** 800
[10] Goksen K, Gasanly N M and Ozkan H 2005 *J. Korean Phys. Soc.* **47** 267
[11] Goksen K, Gasanly N M and Ozkan H 2007 *Acta Phys. Pol.* A **112** 93

[12] Yu P and Cardona M 1996 *Fundamentals of Semiconductors* (Berlin: Springer)
[13] Stadler W, Hofmann D M, Alt H C, Muschik T, Meyer B K, Weigel E, Müller-Vogt G, Salk M, Rupp E and Benz K W 1995 *Phys. Rev.* B **51** 10619
[14] Cotal H L, Lewandowski A C, Markey B G, McKeever S W S, Cantwell E and Aldridge J 1990 *J. Appl. Phys.* **67** 975
[15] Schmidt T, Lischka K and Zulehner W 1992 *Phys. Rev.* B **45** 8989